

庆祝同济大学沈祖炎教授从事钢结构研究50周年

钢结构稳定、 抗震与非线性分析理论

STABILITY, ASEISMIC AND
NONLINEAR ANALYSIS THEORIES
OF STEEL STRUCTURES

——沈祖炎教授论文选集
——Selected Papers of Prof. Shen Zu-Yan

同济大学建筑工程系

中国建筑工业出版社

庆祝同济大学沈祖炎教授从事钢结构研究 50 周年

To Honor Prof. Shen Zu-Yan for His 50 Years of Contributions to Steel Structure Engineering

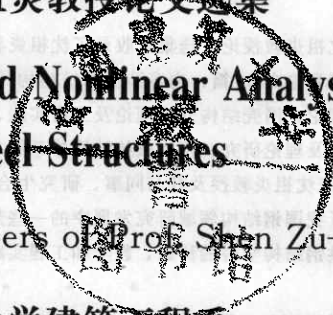
钢结构稳定、抗震与非线性分析理论

——沈祖炎教授论文选集

Stability, Aseismic and Nonlinear Analysis Theories
of Steel Structures

——Selected Papers of Prof. Shen Zu-Yan

同济大学建筑工程系



中国建筑工业出版社

图书在版编目 (CIP) 数据

钢结构稳定、抗震与非线性分析理论/同济大学建筑
工程系. —北京: 中国建筑工业出版社, 2008

ISBN 978-7-112-07275-0

I. 钢… II. 同济大学建筑工程系 III. ①钢结
构-结构稳定性-文集②钢结构-抗震结构-文集③钢结构-
非线性-结构分析-文集 IV. TU391-53

中国版本图书馆 CIP 数据核字(2008)第 018091 号

《沈祖炎教授论文选集》收录了沈祖炎教授在钢结构领域发表的国内
或国际期刊论文 80 篇, 内容涉及钢结构构件稳定理论、高层钢结构分析
及设计理论、网壳结构分析理论及工程实践、新型的钢管桁架结构节点性
能的试验及理论研究、现代张拉结构体系的非线性分析理论。所选论文是
近 20 年来沈祖炎教授及其与同事、研究生合著论文的一部分, 从一个侧
面反映了我国钢结构领域研究发展中的一些热点问题及研究成果。这本论
文集可供钢结构学科的科研、教学和工程实践人员及研究生参考。

* * *

责任编辑: 黎 钟

责任设计: 肖广慧

责任校对: 汤小平

钢结构稳定、抗震与非线性分析理论

——沈祖炎教授论文选集

Stability, Aseismic and Nonlinear Analysis Theories of Steel Structures

——Selected Papers of Prof. Shen Zu-Yan

同济大学建筑工程系

*

中国建筑工业出版社出版 发行(北京西郊百万庄)

各地新华书店、建筑书店经销

北京市铁成印刷厂印刷

*

开本: 787 × 1092 毫米 1/16 印张: 43 字数: 1042 千字

2005 年 5 月第一版 2008 年 6 月第二次印刷

印数: 1000-2500 册 定价: 75.00 元

ISBN 978-7-112-07275-0

(13229)

版权所有 翻印必究

如有印装质量问题, 可寄本社退换

(邮政编码 100037)

序

值同济大学“土木系科”90周年庆典之际，为祝贺我国著名钢结构专家、同济大学资深教授沈祖炎先生从事钢结构研究事业50周年，中国建筑工业出版社将出版这本汇集沈祖炎先生主要科研成果的论文选集，从一个侧面反映沈先生对我国钢结构领域及同济大学钢结构学科发展作出的卓越成就。沈先生曾长期担任同济大学的副校长，分管学校的教学（包括研究生院）、科研和学科规划建设。我在担任同济大学校长之前，曾做过分管教学、科研、外事等的校长助理和副校长，有相当多的时间是在沈先生的指导下工作，他使我比较深入地了解了同济大学学科、专业发展的历程，了解了同济大学严谨求实的优良传统。沈先生治学严谨，作风慎密，我十分敬佩他。很高兴能有机会为他的论文集作序，以表达我的敬佩之情。同时，我也对他在钢结构领域方面所作出的贡献表示衷心的祝贺！

50年来，沈先生在自己的学术领域孜孜不倦，取得了丰硕的研究成果。他先后主持40余项国家及省部级科研项目和20余项重大工程项目的关键问题研究，发表论文300余篇，出版著作近20部，主编和参编的与钢结构有关的规范、规程共11本，获国家级和省部级科技进步奖25项。论文集从5个方面选取了沈先生在钢结构领域发表的论文80篇，内容涉及钢结构构件稳定理论、高层钢结构分析及设计理论、网壳结构分析理论及工程实践、新型的钢管桁架结构节点性能的试验及理论研究、现代张拉结构体系的非线性分析理论。这些研究成果的取得很大程度上提高了我国在钢结构研究及应用领域的理论及实践水平，为中国钢结构学科发展和钢结构工程实践做出了重要贡献。同时，在沈先生的带领下，同济大学钢结构学科无论是在研究梯队建设、研究领域拓展，还是在研究成果、国际合作与交流等方面都取得了令人瞩目的业绩和发展，在国际上也具有较大的影响力。沈先生在土木工程教育方面也做出了重要贡献。他曾连续二届担任全国高等院校土木工程学科专业指导委员会主任及专业评估委员会主任。在此期间，沈先生积极推动国家土木工程专业的评估及评估结果的国际互认和注册结构工程师制度的建立，在教育部面向21世纪土建类人才培养方案和教学体系的研究和实践等方面取得了卓著的成果。

50年来，沈先生身先示范，为人师表，教书育人，桃李天下，是同济大学的一代名师，处处体现了同济大学严谨求实的传统。他值得后辈们崇尚学习。愿同济大学严谨求实的作风代代相传！

衷心祝愿沈祖炎教授身体健康，并在钢结构领域再创辉煌！

中华人民共和国教育部副部长
前同济大学校长

吴启迪

2004年10月

目 录

第一部分 钢结构构件稳定理论

1. Analysis of Initially Crooked, End Restrained Steel Columns	3
2. 单角钢压杆的稳定计算	19
3. Nonlinear Stability Analysis of Steel Members by Finite Element Method	32
4. Interaction of Local and Overall Instability of Compressed Box Columns	48
5. 薄壁轴压焊接方管柱整体稳定-局部稳定相互作用问题的研究	65
6. 受压槽形截面的屈曲后极限强度	74
7. 厚板焊接柱的 φ 曲线研究	83
8. 阶形柱的极限承载力	90
9. 缀板柱稳定极限承载力的数值积分解法	101
10. 对九江长江大桥 15MnVNq 钢重型压杆 φ 曲线的研究	111
11. 对称截面铝合金挤压型材压杆的稳定系数	116
12. 薄壁杆弹塑性弯扭失稳的有限单元解法	125
13. 承受冲击压力的钢压杆	135
14. 结构稳定分析的改进数值积分法	150
15. 钢管结构极限承载力计算的力学模型	161

第二部分 高层钢框架结构静动力极限承载力分析理论

16. Spatial Hysteretic Model and Elasto-Plastic Stiffness of Steel Columns	175
17. 交叉钢支撑滞回特性分析	191
18. 空间钢框架结构的非线性分析	198
19. 空间钢框架结构的弹塑性稳定	207
20. 柔性节点钢框架的二阶弹塑性极限承载力研究	216
21. 空间钢框架结构弹塑性稳定的综合离散分析法	226
22. 考虑塑性区扩展的钢框架二阶分析	235
23. 反复变动轴力作用下钢柱的数值分析模型	240
24. 钢框架受风与地震作用的统一非线性矩阵分析理论	246
25. An Experiment-based Cumulative Damage Mechanics Model of Steel Under Cyclic Loading	255
26. A Hysteresis Model For Plane Steel Members With Damage Cumulation Effects	265
27. 空间钢构件考虑损伤累积效应的恢复力模型及试验验证	272

28. 高层钢结构考虑损伤累积及裂纹效应的抗震分析	279
29. A Synthetic Discrete Method for Analyzing the Elasto-Plastic Seismic Response of Tall Steel Framed-Tube Systems	286
30. Analysis of Nonlinear Behavior of Steel Frames under Local Fire Conditions	295
31. 考虑损伤累积的热弹塑性问题变分原理及其有限元方法	303
32. 灾难性荷载作用下钢结构承载力损伤的数值模拟	310
33. 高温下轴心受压钢构件的极限承载力	316
34. 钢框架结构抗火性能的试验研究	320

第三部分 网壳结构的静动力稳定理论

35. Stability of Single Layer Reticulated Shells	331
36. Improvements on the Arc-Length-Type Method	350
37. 结构非线性分析中求解预定荷载水平的改进弧长法	364
38. 确定结构分支点及跟踪平衡路径的改进弧长法	369
39. 网壳结构分析中节点大位移叠加及平衡路径跟踪技术的修正	374
40. 节点大位移条件下的梁—柱单元坐标转换矩阵	381
41. 稳定分析中极值点失稳与分枝点失稳的跟踪策略及程序实现	387
42. 扰动法在结构分枝失稳分析中的应用	394
43. 平面梁杆结构几何非线性分析的一种简便方法	401
44. 大跨度拱支网壳结构的弹塑性分析理论及程序编制	406
45. 网壳结构节点体对其承载性能的影响	413
46. 单层网壳结构弹塑性稳定试验研究	418
47. Arch-Supported Reticulated Shell Structures and Their Static Mechanical Behaviour	427
48. 大型空间结构整体模型静力试验的若干关键技术	437
49. 上海东方明珠国际会议中心单层球网壳整体模型试验研究	444
50. 运动稳定性理论在结构动力分析中的应用	452
51. 杆系钢结构非线性动力稳定性识别与判定准则	459
52. 广义位移控制法在动力稳定问题中的应用	464
53. 单层鞍型网壳在地震作用下的动力稳定分析	469
54. 初始缺陷对网壳结构动力稳定性能的影响	475
55. 钢网壳模型的动力稳定性振动台试验研究	481
56. Shaking Table Tests of Two Shallow Reticulated Shells	488

第四部分 钢管桁架直接汇交节点承载力试验和理论分析

57. 圆钢管节点的强度计算公式	501
58. 关于直接汇交钢管节点的焊缝计算	506
59. 焊接方管节点极限承载力计算	519

60. 钢结构焊接方管节点疲劳性能研究	525
61. 方管焊接节点的疲劳强度	532
62. 直接汇交节点三重屈服线模型及试验验证	539
63. 双向贯通式钢管节点力学性能的试验研究	547
64. 圆钢管相贯节点滞回特性的试验研究	553
65. 空间结构大型铸钢节点试验研究	561
66. 矩形钢管屋架的试验研究	566
67. 上海市八万人体育场屋盖的整体模型和节点试验研究	571

第五部分 张拉结构非线性分析理论

68. 预应力索结构中的索单元数值模型	583
69. 悬索结构非线性分析的滑移索单元法	589
70. 索穹顶结构非线性分析的曲线索单元有限元法	597
71. 张力结构的非线性有限元分析	603
72. 索网结构几何非线性分析的增量理论	611
73. 索穹顶结构的静力性状分析	617
74. 圆形平面轴对称索穹顶结构成形后的刚度计算	625
75. 基于非线性有限元的索穹顶施工模拟分析	632
76. 索穹顶结构成形试验研究	640
77. 斜拉网壳结构构件单元分析及结构动力性能	645
78. 斜拉网壳结构的非线性地震响应特性	653
79. 上海浦东国际机场候机楼 R2 钢屋架足尺试验研究	659
80. 上海浦东国际机场 R2 钢屋盖模型模拟三向地震振动台试验研究	668

第一部分

钢结构构件稳定理论

1. Analysis of Initially Crooked, End Restrained Steel Columns

Zu-Yan Shen and Le-Wu Luv

Synopsis

Abstract: A new and general method of analysis for steel columns, which can simultaneously take into account the effects of initial crookedness, end restraint, residual stress and load eccentricity, has been developed. The method gives the complete load-deflection relationship of a column, including both the ascending and descending branches. Unlike most of the currently used methods, the basic required input is the stress-strain relationships of the material, instead of some pre-determined moment-thrust-curvature relationships for the cross sections. Application is first made to develop theoretical predictions for some selected columns which were tested using either the geometrical alignment or the load alignment procedure. It is shown that the latter tends to be stronger and gives a higher test load. The results of two parametric studies, which included such variables as magnitude of initial crookedness, amount of end restraint, pattern of residual stress distribution, and axis of bending, are also presented. Certain conclusions with regard to the relative importance of these variables are drawn.

Notation

A cross-sectional area	v initial crookedness of column
E modulus of elasticity	w deflection of column
e eccentricity	y distance from centroidal axis
I moment of inertia	z distance from end A
K effective length factor	β ratio of eccentricity at end A to that at end B
L length of column	ϵ strain
M bending moment	θ slope of deflected column
N normal force at section	λ non-dimensional slenderness ratio
P axial load	σ stress
R rotational stiffness of end restraint	ϕ curvature
r radius of gyration	
V end reaction	

1 Introduction

Among the various factors that affect the strength of a column in a framework, the

following are considered to be important: (i) initial crookedness, (ii) end restraint, (iii) residual stress, and (iv) eccentricity of applied load. Past research has paid much attention to the effects of initial crookedness and residual stress. A thorough study of all these factors, however, is considered as essential in the development of rational design provisions for columns.

Figure 1 shows an initially crooked and end restrained column of length L . The crookedness v varies with the distance z from the left-hand end. The modulus of elasticity of the material is E , and the moment of inertia of the cross section is I . An eccentric load P is applied with eccentricities e_a and e_b , and produces deflection w . The stiffness of the end restraints, which are represented by springs, are R_a and R_b , and the restraining moments acting at the two ends are $R_a\theta_a$ and $R_b\theta_b$, where θ_a and θ_b are the end rotations produced by the load P . For the numerical studies to be described later it has been found convenient to specify R_a and R_b nondimensionally in terms of EI/L of the column.

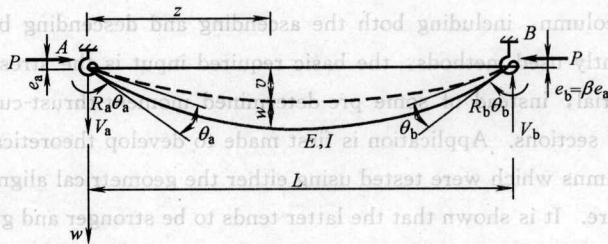


Fig. 1 Initially crooked, end restrained column

Consider first the case where the axial load is concentrically applied, that is, $e_a = e_b = 0$. Several possible load-deflection curves for the column are shown in Figure 2, where v_m and w_m represent, respectively, the initial crookedness and deflection at the mid-height. If the column is perfectly straight ($v_m = 0$) and without end restraint ($R = 0$), buckling will take place when the applied load reaches the tangent modulus load of a pin-ended column. The behaviour of the column is represented by curve (a). The load eventually reaches a maximum value at which the column fails by inelastic instability. If the

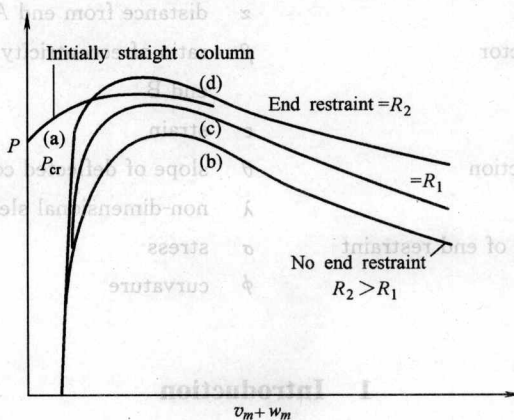


Fig. 2 Load-deflection behaviour of concentrically loaded column

column has an initial crookedness v_m , deflection w_m will take place as soon as the first load is applied and will increase continuously. This behaviour is shown as curve (b). Failure of the column is again due to inelastic instability, but occurring at a reduced maximum load. This reduction is dependent on the magnitude of v_m . When the column is partially restrained at the ends ($R=0$), its load-deflection relationship is represented by curve (c) or (d). For sufficiently large values of R , the ultimate strength of the crooked column can exceed that of the straight column.

Next, consider the case when the load is applied with an eccentricity e , equal at both ends; that is, $e_a = e_b = e$ (Figure 3). The column is initially crooked and unrestrained. If the eccentricity e and the crookedness v_m are on opposite sides of the straight line connecting the column ends ($e = -e_1$), there will be a reduction in the column strength due to the added moment Pe_1 . On the other hand, if e and v_m are on the same side ($e = +e_1$), the strength of the column may be enhanced by the moment Pe_1 , which acts in the direction opposite to that of the Pv moment. At a larger eccentricity, for example $e = +e_2 > e_1$, the counteracting moment Pe_2 may be sufficient to force the column to deflect, and eventually fail, in the direction opposite to the initial crookedness. This phenomenon has been observed in previously reported column tests.

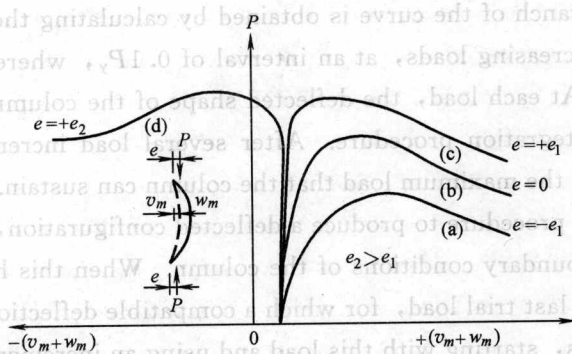


Fig. 3 Load-deflection behaviour of eccentrically loaded column

2 Method of analysis

A general method, which can take into account almost all the known factors affecting column behaviour, has been developed to perform load-deflection analyses of columns. The specific factors that are included in the development are:

- (i) Initial crookedness
- (ii) End restraints
- (iii) Residual stresses
- (iv) Load eccentricities
- (v) Variation in mechanical properties of material over cross section
- (vi) Stress-strain characteristics of material
- (vii) Loading, unloading and reloading of yielded fibres.

Any pattern of residual stress distribution and any variation of initial crookedness along the length of the column can be incorporated. The restraints and eccentricities may be equal or unequal at the two ends. By allowing a variation in the mechanical properties over the cross section, it is possible to include hybrid columns or columns with non-uniform strength properties. Any type of stress-strain relationship, such as bi-linear, tri-linear and non-linear can be included in the analysis. The bi-linear and tri-linear relationships are commonly used for steel columns, with the option of including the effect of strain hardening. A major difference between the method presented in this paper and those employed previously in analysing crooked columns or beam-columns is that it does not use any pre-determined moment-thrust-curvature ($M-P-\phi$) curves in the integration process. The basic input is the stress-strain relationship and the necessary $M-P-\phi$ relationships are generated internally as needed. The stress history of all the elements in a cross section is carefully followed, and any occurrence of unloading or reloading of the yielded elements can be detected and its effect is included in the generation of the $M-P-\phi$ relationships. The method makes no assumption with regard to the shape of the initial crookedness or of the deflected column under load. The analysis gives both the ascending and descending branches of the load-deflection curve.

The ascending branch of the curve is obtained by calculating the deflections for a series of successively increasing loads, at an interval of $0.1P_y$, where P_y is the axial yield load of the column. At each load, the deflected shape of the column is determined by an iterative numerical integration procedure. After several load increments, the trial load will eventually exceed the maximum load that the column can sustain. This is indicated by failure of the iterative procedure to produce a deflected configuration, which is compatible with the prescribed boundary conditions of the column. When this happens, the calculation is returned to the last trial load, for which a compatible deflection has been found. A new set of calculations, starting with this load and using an increment of $0.01P_y$, is then carried out. Once again the successive calculations eventually will show a stable load (below the maximum), and an unstable load (above the maximum), with a difference of $0.01P_y$. This means the stable load is now within $0.01P_y$ of the maximum load. The entire process is repeated again with the size of the load increment reduced to $0.001P_y$ and eventually to $0.0001P_y$.

To obtain the load-deflection curve of the column beyond the maximum load, the same method can still be applied except that the analysis must now be performed by using deflection increments. In actual calculations, however, it has been found to be more convenient to use increments of end rotation. For each selected end rotation, an equilibrium load is found using the same iterative procedure.

Referring to the column shown in Figure 1, the equations of equilibrium for any section located at a distance z from the left end are:

$$M = P(e_a + v + w) - R_a \theta_a - V_a z \quad (1)$$

and

$$(11) \quad V_a - N = P \quad (2)$$

in which M and N are, respectively, the bending moment and axial force acting on the section, and V_a the reaction at end A. This reaction is given by

$$(12) \quad V_a = [Pe_a(1-\beta) - (R_a\theta_a - R_b\theta_b)]/L \quad (3)$$

in which β is the eccentricity ratio, e_b/e_a . Equilibrium requires that M and N be equal to the internal resisting moment and axial force of the section, which can be calculated by integrating the normal stress σ over the cross section (positive for compression). Thus,

$$(13) \quad M = \int_A \sigma y dA \quad (4)$$

and



$$(14) \quad N = \int_A \sigma dA \quad (5)$$

in which y is the distance from dA to the centroidal axis of the cross section.

The stress σ acting on the element dA is a function of the strain ϵ

$$(15) \quad \sigma = f(\epsilon) \quad (6)$$

ϵ consists of three parts

$$(16) \quad \epsilon = \epsilon^r + \epsilon^p + \phi y \quad (7)$$

in which ϵ^r is the residual strain, ϵ^p the strain at the centroid or the axial strain (in the elastic range $\epsilon^p = P/AE$), and ϕ the curvature. Equations 1 to 7 are the fundamental equations of the problem.

For a given load P , the deflected shape of the column, defined by the end rotations θ_a and θ_b , is sought. A value of θ_a is first assumed (for columns with unsymmetrical restraints both θ_a and θ_b must be assumed) and numerical integration is then carried out to determine the deflected shape for the assumed θ_a (Figure 4). The procedure adopted is similar to the one developed previously for analysing laterally loaded beam-columns.⁽¹⁾ The column is divided into many short segments and the deflection and the slope at the end (nodal point) of each segment are calculated by numerical integration. Suppose that the calculation has reached nodal point $n-1$, the deflection w_{n-1} , the slope θ_{n-1} , the bending moment M_{n-1} , the curvature ϕ_{n-1} , and the axial strain ϵ_{n-1}^p have all been calculated. For the next segment whose length is ΔL_n , the following approximate formulae can be used to calculate the deflection and the slope at point n

$$(17) \quad w_n = w_{n-1} + \theta_{n-1} \Delta L_n - \frac{1}{2} \phi_{n-1/2} \Delta L_n^2 \quad (8)$$

and

$$(18) \quad \theta_n = \theta_{n-1} + \phi_{n-1/2} \Delta L_n \quad (9)$$

in which $\phi_{n-1/2}$ is the curvature at the mid-point $n-1/2$ of the segment. This curvature, yet to be determined, is a function of the bending moment and the axial force acting at $n-1/2$, which, according to equations 1 and 2, are given by

$$(19) \quad M_{n-1/2} = P(e_a + v_{n-1/2} + w_{n-1/2}) - R_a\theta_a - V_a z_{n-1/2} \quad (10)$$

and

$$N_{n-(1/2)} = P \quad (11)$$

The deflection at $n-1/2$ is

$$w_{n-(1/2)} = w_{n-1} + \theta_{n-1} \frac{\Delta L_n}{2} - \frac{1}{2} \phi_{n-(1/2)} \left(\frac{\Delta L_n}{2} \right)^2 \quad (12)$$

Substituting equation 12 into equation 10 results in the following expression for $\phi_{n-(1/2)}$

$$\phi_{n-(1/2)} = \frac{2\{e_a + v_{n-(1/2)} + w_{n-1} + \theta_{n-1}(\Delta L_n/2) - [(R_a \theta_a + V_a z_{n-(1/2)})/P] - (M_{n-(1/2)}/P)\}}{[(\Delta L_n)^2/2]} \quad (13)$$

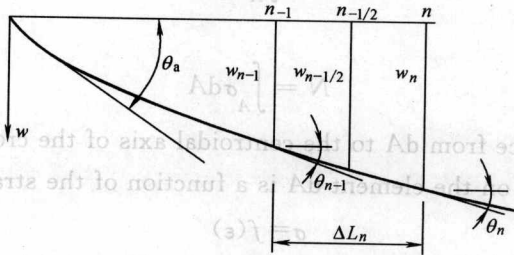


Fig. 4 Segment of a deflected column

It is apparent from equations 10 to 13 that a direct solution of $\phi_{n-(1/2)}$ is not possible, and an iterative procedure must therefore be devised. Trial values of $\phi_{n-(1/2)}$ and $\epsilon_{n-(1/2)}^p$ are first assumed (convenient trial values would be the known ϕ_{n-1} and ϵ_{n-1}^p from the previously-completed calculations) and the total strain ϵ at any point in the cross section is calculated from equation 7 and the corresponding stress σ from equation 6. With σ known, equation 4 can then be used to calculate the bending moment $M_{n-(1/2)}$. Because of the complex patterns of residual strain present in most structural shapes, the required integration of equation 4 is best performed numerically by subdividing the cross section into a large number of small elements. Each element is assumed to have a uniform residual strain ϵ^r and total strain ϵ . The stress σ_j acting on each element with an area of ΔA_j is determined from equation 6 for the total strain ϵ_j . Equation 4 now assumes the following form

$$M = \sum_j \sigma_j y_j \Delta A_j \quad (14)$$

which can be applied to calculate the desired bending moment at $M_{n-(1/2)}$. Substitution of $M_{n-(1/2)}$ into equation 13 gives a new value of $\phi_{n-(1/2)}$ which is to be compared with the assumed $\phi_{n-(1/2)}$. If the two values do not agree, the above process must be repeated. Satisfactory agreement is reached if the assumed and calculated values differ by less than 0.5 percent. The $\phi_{n-(1/2)}$ value thus determined satisfies equations 10 and 13. It should be remembered that the axial strain $\epsilon_{n-(1/2)}^p$ was also assumed at the beginning of the iterative calculation. This strain is related to the axial force $N_{n-(1/2)}$ which must satisfy equation 11. It is, therefore, necessary to check if the stresses σ_j associated with the $\phi_{n-(1/2)}$ satisfy equation 11. This can be done by substituting the σ_j values into equation 15, whose

form is

$$N = \sum_j \sigma_j \Delta A_j \quad (15)$$

If $N_{n-(1/2)}$ is not equal to the axial force P as required by equation 11, a new $\epsilon_{n-(1/2)}^p$ must be selected and the process of calculation is repeated (including the iterative calculation performed previously to obtain $\phi_{n-(1/2)}$). Satisfactory convergence is obtained if the calculated $N_{n-(1/2)}$ is within $0.00001P_y$ of the axial load. When this occurs, the search for the correct values of $\phi_{n-(1/2)}$ and $\epsilon_{n-(1/2)}^p$ is complete, and the corresponding $\phi_{n-(1/2)}$ can be substituted into equations 8 and 9 to determine w_n and θ_n at nodal point n . This completes all the required calculations for the segment ΔL_n .

The same calculation is repeated for all the remaining segments. When the calculation for the last segment is completed, the result, if not equal to zero, may show a vertical displacement w_b at end B . A non-zero w_b indicates that a new θ_a should be tried. It is convenient to select the new θ_a to be equal to the initial θ_a minus w_b/L if w_b is a downward displacement, or θ_a plus w_b/L if w_b is an upward displacement. The entire integration is then repeated, and another w_b is found. Using the two w_b values and the corresponding θ_a values, a third θ_a can be selected by linear interpolation and the integration again repeated. Further repetitions of the process may be required, each time resulting in an improved θ_a . The correct θ_a and therefore the correct deflected shape of the column is found if w_b/L at the end of the calculations is less than $1/1000$ of the assumed θ_a .

A comprehensive computer program for performing all the numerical calculations with the various convergence criteria stated previously has been prepared. In this program, the column may be divided into any number of equal or unequal segments. For the study presented in this paper the columns have been divided into seven equal segments with eight nodal points.

3 Analytical prediction of test column behaviour

The method is first applied to generate the load-deflection curves of some pin-ended columns which were tested in previous studies at Lehigh University. The purpose of this work is twofold: (i) to obtain experimental verification of the analysis method, and (ii) to develop analytical predictions for selected columns whose behaviour has not previously been substantiated by theory. The columns selected had varying amounts of initial crookedness which were carefully measured before testing. Included are: two concentrically loaded columns, one eccentrically loaded column with small positive eccentricity, and one eccentrically loaded column with large positive eccentricity.

The concentrically loaded columns are selected from a group of heavy European columns which were tested as part of a co-operative study with the European Convention for Constructional Steelwork (ECCS). The procedure adopted for these tests followed the ECCS recommendations which require the test column to be 'geometrically aligned' with

respect to the centreline of the testing machine. The test load was applied continuously to the column at a prescribed rate, and the 'dynamic' load-deflection curve was recorded automatically as the test progressed. The results of the tests have already been published,⁽²⁾ but no attempt has yet been made to provide theoretical predictions. Figure 5 shows comparisons of the analytical and experimental load-deflection curves of the two HEM 340 columns manufactured in Italy. All the analyses are based on the dynamic stress-strain characteristics determined from the tension coupon tests and the measured residual stresses and initial crookedness. For each test column, two analyses have been performed: one includes the effect of strain hardening (dashed line) and the other neglects it (dot-dashed line). When the two analyses gave essentially the same results, the one that includes the effect of strain hardening is shown. For the two columns the analytical predictions show remarkably good agreement with the test results. For the column with $L/r = 50$, the effect of strain hardening becomes quite pronounced after the attainment of the maximum load. On the other hand, strain hardening appears to have very little effect on the behaviour of the column with $L/r = 95$ because the two analyses gave almost the same load-deflection curve. This study also shows that it is possible to develop the dynamic load-deflection relationship of a test column by using the dynamic mechanical properties if the strain rate in the column test is not too different from the strain rate specified in the coupon test.

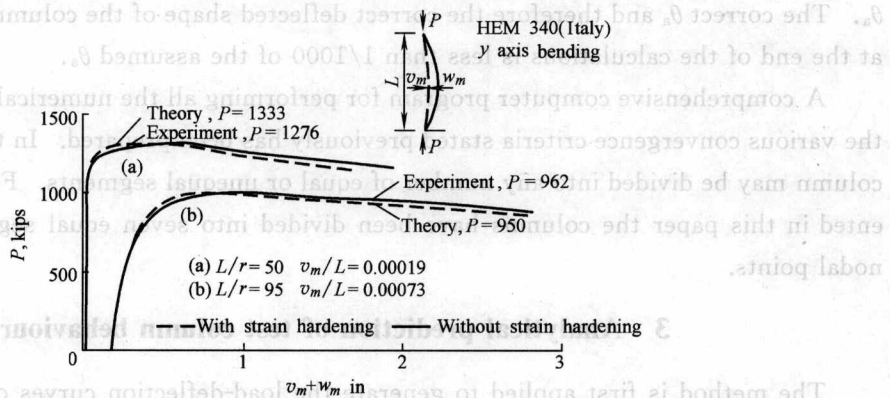


Fig. 5 Analytical and experimental load-deflection curves of concentrically loaded columns

An example of an eccentrically loaded column with small positive eccentricity is shown in Figure 6. The column is a welded H column with A514 steel flanges and A36 steel web and was included in a pilot programme studying hybrid columns.⁽³⁾ Before testing, the column was aligned under load by the so-called 'old Lehigh method'. The goal of the alignment was to achieve a reasonably uniform strain distribution in the column during the early stages of testing. If the column is initially crooked, in order to achieve uniform distribution, the alignment load as well as the test load must be applied eccentrically. For the selected column, the results given in Figure 6 show that the strength of the column was increased from $0.652P_y$ for $e/L = 0$ to $0.745P_y$ for $e/L = 0.000469$, which is the value of eccentricity adopted in the calculation. This value of e has been determined in such a